Polar Biology
https://doi.org/10.1007/s00300-019-02564-7

ORIGINAL PAPER

Phytoplankton composition and bloom formation in unexplored nearshore waters of the western Antarctic Peninsula

Martina Mascioni[1,2] · Gastón O. Almandoz[1,2] · Adrián O. Cefarelli[3,4] · Allison Cusick[5] · Martha E. Ferrario[1,2] · Maria Vernet[5]

Received: 14 January 2019 / Revised: 27 June 2019 / Accepted: 22 August 2019

Abstract

The western Antarctic Peninsula (WAP) is one of the most productive regions in the Southern Ocean. However, little is known about the phytoplankton composition in nearshore waters, in fjords and channels between 63° and 67°S, where Antarctic krill and baleen whales are conspicuous. This study represents the first attempt to describe spatial and temporal composition of the phytoplankton community (species, cell concentration, phytoplankton biomass) in twelve relatively unexplored nearshore sites of the WAP. Sampling was carried out in the frame of a Citizen Science project during late summer of 2016 and during the spring–summer 2016–2017. Species identification and enumeration were performed by light and scanning electron microscopy and phytoplankton carbon biomass was estimated by using cell-volume conversion. The highest phytoplankton abundance and biomass values were found in December-January, and were mainly represented by nanophytoflagellates (2–20 µm). Cryptophytes were more abundant in early summer and prasinophyceans in late summer. The abundance of large bloom-forming diatoms was unexpectedly low. Three blooming flagellated taxa were found during the sampling season, chronologically: *Pyramimonas* sp. in Neko Harbor (March 3, 2016, 1.4×10^6 cells L^{-1}, and 327 µgC L^{-1}), cryptophytes in Wilhelmina Bay (December 14, 2016, 6.4×10^6 cells L^{-1}, and 97.5 µgC L^{-1}) and unidentified unarmored dinoflagellates near Danco Island (December 18, 2016, 9.5×10^6 cells L^{-1}, and 1597 µgC L^{-1}). The last one represents, as far as we know, the first record of a dinoflagellate bloom in the WAP. It is to note that blooming organisms, analyzed morphologically, do not coincide with previously described Antarctic species.

Keywords Western Antarctic Peninsula · Citizen Science · Diatoms · Cryptophyta · *Pyramimonas* sp. · Unarmored dinoflagellate bloom

Introduction

The western Antarctic Peninsula (WAP) continental shelf includes the most extensive system of glacio-marine fjords of the Antarctic continent. Ecological and biogeochemical processes in these ecosystems are strongly influenced by sea ice formation and freshwater input from melting glacial ice and sea ice (Dierssen et al. 2002; Meredith et al. 2008, 2016; Ducklow et al. 2013). Recently, the WAP has undergone rapid climate warming, linked to diminished sea ice extent and duration and increasingly importance of glacial discharge to the ocean (Meredith and King 2005; Cook et al. 2016; Meredith et al. 2016). In general, productivity and phytoplankton biomass (Chlorophyll *a*) increase towards the coast (Smith et al. 2008), in association with shallow mixed layers (Vernet et al. 2008). Particularly, in these WAP embayments, baleen whales, seals and penguins

✉ Martina Mascioni
marmascioni@gmail.com

1 División Ficología, Facultad de Ciencias Naturales y Museo, Universidad Nacional de La Plata, Paseo del Bosque s/n, 1900 La Plata, Argentina

2 Consejo Nacional de Investigaciones Científicas y Técnicas (CONICET), Godoy Cruz 2290, C1425FQB Ciudad Autónoma de Buenos Aires, Argentina

3 Instituto de Desarrollo Costero, Universidad Nacional de la Patagonia San Juan Bosco, Ruta Provincial 1 km 4, 9005 Comodoro Rivadavia, Argentina

4 Centro de Investigaciones y Transferencia Golfo San Jorge, CONICET, Ruta Provincial 1 km 4, 9005 Comodoro Rivadavia, Argentina

5 Integrative Oceanography Division, Scripps Institution of Oceanography, University of California San Diego, La Jolla, CA 92093-0218, USA

Published online: 05 September 2019

feed on small invertebrates (i.e., krill, copepods, salps) that depend on phytoplankton for their survival (Montes-Hugo et al. 2009; Nowacek et al. 2011). Diatoms are known to bloom at the sea ice edge and coastal environments (Garibotti et al. 2003a; Ducklow et al. 2013). However, due to climate warming over the past 40 years, a change in the food web has been detected, triggered mainly by a replacement in phytoplankton from microplanktonic diatoms (≥ 20 µm) to nanoflagellates (< 20 µm) (Moline et al. 2004; Montes-Hugo et al. 2009; Mendes et al. 2013; Schofield et al. 2017 but see Schloss et al. 2014; Höfer et al. 2019).

In southern Bransfield and Gerlache Straits, phytoplankton is dominated by nano- and picoplankton (< 2 µm) throughout most of the year. Blooms of diatoms, prymnesiophytes (*Phaeocystis antarctica*), prasinophyceans (*Pyramimonas* sp.) and cryptophytes are a recurrent phenomenon during spring and summer (Vernet et al. 1991; Ferrario and Sar 1992; Rodriguez et al. 2002; Varela et al. 2002; Schofield et al. 2017; Mendes et al. 2018, among others). Seasonal and interannual variability in bloom magnitude is high (Rodriguez et al. 2002; Garibotti et al. 2003a, 2005; Mendes et al. 2013). However, it is not known if the phytoplankton from the WAP nearshore waters, in particular within fjords, are similar to the shelf and other coastal communities between 63° and 65°S. Phytoplankton in these nearshore waters (e.g., Neko Harbor, Wilhelmina Bay, Hanusse Bay, Fig. 1) have been rarely studied. Two previous studies provided description and enumeration of diatoms collected from net tows (May et al. 1991; Ferrario et al. 1998) but were unable to inform about nanoflagellates. The high megafaunal congregation within these fjords (Nowacek et al. 2011; Grange and Smith 2013) highlights the importance of documenting these poorly known phytoplankton communities.

In this study, we analyze spring–summer phytoplankton biomass and composition in the relatively unexplored fjords and passages of the WAP in order to compare the species composition and abundance of nano- and microplankton observed with previous reports in shelf and other coastal waters within the Peninsula region (i.e., Anvers Island, Bransfield, and Gerlache straits).

Materials and methods

Phytoplankton sampling was carried out in the frame of a Citizen Science project, FjordPhyto (www.fjordphyto.org). The samples were collected during Antarctic cruises operated by two tourism companies, G Adventures and Polar Latitudes, both members of the International Association of Antarctica Tour Operators (IAATO).

The sampled area comprised the west coast of the Antarctic Peninsula between 63°54′18.00″ and 66°53′12.03″ South and 60°46′44.40″ and 67°53′45.36″ West (Fig. 1).

A total of 41 samples, from 12 sampling areas (Fig. 1), were collected. The sampling period included a first survey in February–March 2016 in Neko Harbor (3 samples, Table 1) and the austral spring–summer 2016–2017, from November to March (38 samples, Table 1). Surface samples were collected aboard a Zodiac by submerging 120-mL bottles in the water by hand to approximately 25 cm depth, to avoid sampling the superficial layer. Subsequently, samples were fixed with Lugol's solution at 4% (Edler and Elbrächter

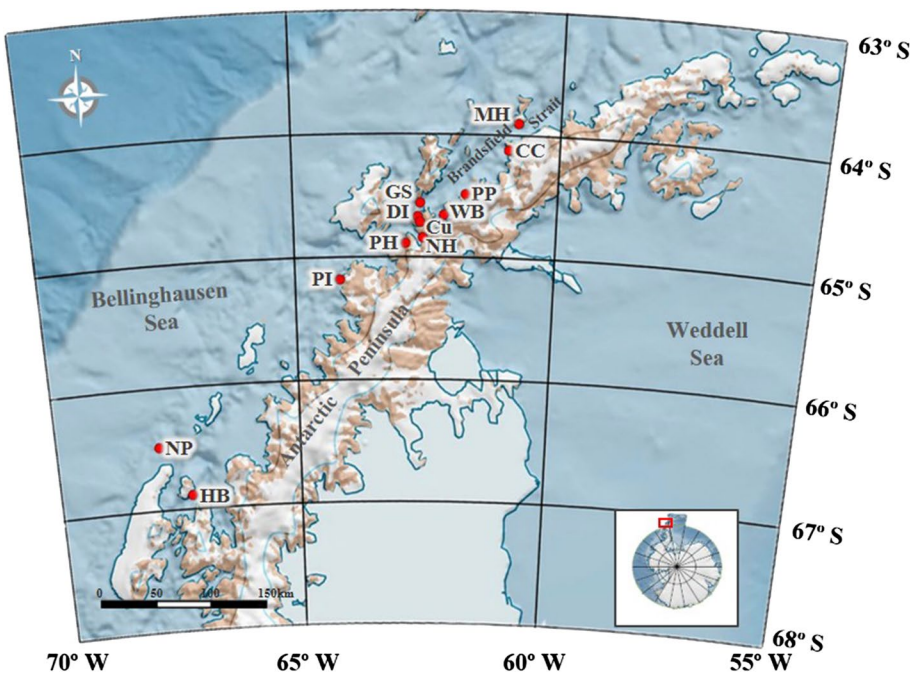

Fig. 1 Location of the twelve main sampling areas in the western coast of the Antarctic Peninsula. Names are abbreviated as follow: Mikkelsen Harbor (MH), Cierva Cove (CC), Portal Point (PP), Gerlache Strait (GS), Wilhelmina Bay (WB), Danco Island (DI), Cuverville (Cu), Neko Harbor (NH), Paradise Harbor (PH), Peterman Island (PI), New Position (NP) and Hanusse Bay (HB)

Table 1 Detail of the sampling area, date and location of the 41 samples from 2016 to 2017, organized according to the day of the month

ID number	Station	Sampling date	Latitude (S°)	Longitude (W°)
1	Cuverville	16-Nov-16	64°40′04.8″	62°37′48″
2	Cierva cove	18-Nov-16	64°09′18″	60°55′12″
3	Mikkelsen Harbor	18-Nov-16	63°54′18″	60°46′44.4″
4	Cierva cove	24-Nov-16	64°08′00.24″	60°55′42.3″
5	Portal Point	24-Nov-16	64°29′13.26″	61°43′49.26″
6	Wilhelmina Bay	25-Nov-16	64°37′13.44″	62°12′07.14″
7	Wilhelmina Bay	8-Dec-16	64°39′24.84″	62°08′08.16″
8	Danco Island	10-Dec-16	64°42′59.04″	62°35′18.96″
9	Portal Point	14-Dec-16	64°29′13.26″	61°43′49.26″
10	Wilhelmina Bay	14-Dec-16	64°37′13.44″	62°12′07.14″
11	Neko Harbor	17-Dec-16	64°50′34.44″	62°32′13.13″
12	Cuverville	17-Dec-16	64°40′12.12″	62°38′24.72″
13	Danco Island	18-Dec-16	64°42′58.79″	62°35′18.85″
14	Cierva cove	23-Dec-16	64°08′12″	60°56′48″
15	New Position	25-Dec-16	66°29′00.78″	67°53′45.36″
16	Cuverville	26-Dec-16	64°40′00.12″	62°38′36″
17	Neko Harbor	26-Dec-16	64°50′21.6″	62°32′19.8″
18	Paradise Harbor	27-Dec-16	64°53′15″	62°51′50.58″
19	Gerlache Strait	29-Dec-16	64°33′36″	62°35′24″
20	Cierva cove	2-Jan-17	64°07′18″	60°57′24″
21	Wilhelmina Bay	4-Jan-17	64°40′24″	62°06′30″
22	Cuverville	6-Jan-17	64°40′18.3″	62°38′06.3″
23	Paradise Harbor	8-Jan-17	64°53′18.3″	62°52′03.66″
24	Danco Island	8-Jan-17	64°43′47.4″	62°36′31.2″
25	Neko Harbor	12-Jan-17	64°50′34.2″	62°32′16.2″
26	Wilhelmina Bay	20-Jan-17	64°42′58″	62°15′26″
27	Neko Harbor	20-Jan-17	64°50′31″	62°32′13″
28	Cuverville	3-Feb-17	64°40′23.34″	62°37′39.54″
29	Neko Harbor	3-Feb-17	64°50′06″	62°32′03.06″
30	Paradise Harbor	5-Feb-17	64°53′01.2″	62°53′34.8″
31	Neko Harbor	9-Feb-17	64°50′33″	62°32′04″
32	Neko Harbor	12-Feb-17	64°50′22.92″	62°32′06.72″
33	Neko Harbor	14-Feb-16	64°49′59.88″	62°33′00″
34	Hanusse Bay	16-Feb-17	66°53′12.03″	67°16′43.26″
35	Neko Harbor	17-Feb-17	64°50′30″	62°32′09″
36	Peterman Island	17-Feb-17	65°10′56.67″	64°08′12.36″
37	Cierva cove	20-Feb-17	64°07′26″	60°56′44″
38	Neko Harbor	22-Feb-16	64°49′59.88″	62°33’00″
39	Cierva cove	27-Feb-17	64°07′26″	60°56′44″
40	Neko Harbor	1-Mar-17	64°50′25.2″	62°32′23.82″
41	Neko Harbor	3-Mar-16	64°49′59.88″	62°33′00″

2010) and kept in a cool dark location. Cruise field guide staff received in-person training from Citizen Science project researchers on appropriate sampling methods before the start of each season. At the end of the season, samples were sent to the lab in the Phycology Division of the Faculty of Natural Sciences and Museum of the National University of La Plata (Argentina) for analysis. The samples were analyzed a year after its collection.

Cell counts were performed according to Utermöhl (1958) using an inverted optical microscope Leica DMIL LED. Subsamples of 50 mL were left to settle for 24 h in a composite sedimentation chamber. At least 100 cells of the dominant taxa were counted at the maximum amplification (×400) (Lund et al. 1958). The whole chamber bottom was also scanned at 200× to count large and sparse species. Additionally, individual specimens from bloom species were

picked by a micropipette and examined under an optical microscope (OM) (Leica DM 2500) with phase contrast and differential interference contrast to make further qualitative observations (pyrenoids, flagella, etc.).

Cell dimensions were measured by using an ocular micrometer. At least 20 randomly selected cells were measured for each of the most abundant species, while 10–15 specimens were generally considered for the rest, following Hillebrand et al. (1999). Cell biovolumes were calculated by approximation to the nearest geometric shapes as proposed by Hillebrand et al. (1999) and Sun and Liu (2003). Cell carbon content (C) was estimated with two different carbon to volume ratios, one for diatoms and one for all other algae groups (Menden-Deuer and Lessard 2000).

For the observations with scanning electron microscope (SEM), sample aliquots from ID# 8, 10, 13, 24, 27, 41 (Table 1) were filtered onto 0.2 µm polyamide filters and dehydrated through an ethanol dilution series (25%, 50%, 75%, 100%) with final critical point dehydration. Specimens were sputter-coated gold–palladium and then examined with two electron microscopes, a Jeol JSM-6360 LV (Facultad de Ciencias Naturales y Museo, Universidad Nacional de La Plata) and a Carl Zeiss NTS SUPRA 40 (Centro de Microscopía Avanzada, Universidad de Buenos Aires).

The software QGIS (2.18, 2016) was used to make the distribution maps.

Results

Phytoplankton biomass and composition

Total phytoplankton abundance varied significantly in the entire sampled season (Table 2, Fig. 2a). The highest concentrations ($> 2.5 \times 10^6$ cells L^{-1}) were recorded between December and January, with lower abundances in November, February, and March (Figs. 2a and 3a). The highest concentrations were observed between Wilhelmina Bay and Paradise Harbor (Fig. 2a). Total biomass varied by three orders of magnitude (Table 2) with higher values between December and March (Figs. 2b and 3a). The highest biomass (1686.8 µgC L^{-1}) was found in December in Danco Island during an unarmored dinoflagellate bloom (sample 13). High biomass (100–650 µgC L^{-1}) was observed also during December and January in 2016–2017 between Portal Point and Neko Harbor (between 64° 29′ and 64° 50′S), coincident with the area of greatest cellular abundance, further south in February around Hanusse Bay and in March 2016 in Neko Harbor when a *Pyramimonas* sp. bloom took place (sample 41).

Dinoflagellates and diatoms were the most important groups in terms of carbon biomass contribution throughout the study period (Fig. 3c), representing 58.4 and 30.8% of total carbon, respectively. They were followed by cryptophytes (5%), prasinophyceans (4.4%), and small unidentified flagellates (1.4%) (Fig. 3c). Small unidentified flagellates (≤ 5 µm) dominated the entire-season phytoplankton abundance (41%) followed by diatoms (25%), cryptophytes (24%), dinoflagellates (8%), and prasinophyceans (2%) (Fig. 3b).

Dinoflagellates were present in the entire season but were more conspicuous during December when they reached the highest abundance and biomass (Table 2, Fig. 3). They were also important during February and March and were at a minimum during November (Table 2, Fig. 3c). The group was mainly represented by unarmored and relatively small species (between 5 and 20 µm), which accounted for 83% of total dinoflagellate abundance and almost 60% of total dinoflagellate biomass (data not shown). Armored dinoflagellates of the genera *Oxytoxum*, *Peridiniella*, *Prorocentrum*, and *Protoperidinium* were usually observed in lower abundance and contributed less to biomass.

Diatoms were present in all stations and were usually found in low concentrations (Table 2). During the entire study period, diatoms contributed mainly to the phytoplankton total carbon in samples with medium to low biomass (Fig. 3a, c). Small and large diatoms contributed differently to abundance and biomass. Highest diatom biomass values (248 and 357 µgC L^{-1}) corresponding to abundances of 1.7 and 2.1×10^5 cells L^{-1} were found during February 2016 in Neko Harbor (samples 33 and 38 respectively), and *Odontella weissflogii* was the most abundant diatom in those samples (64-76% of total diatom abundance). In February 2017, only in the southernmost

Table 2 Maximum, minimum and average values of cell abundance (cells L^{-1}) and biomass (µgC L^{-1}) of the main phytoplankton groups observed throughout the entire sampling season

	Total Phytoplankton		Cryptophytes		Prasinophyceans		Small flagellates		Diatoms		Dinoflagellates	
	Cells	Biomass	Cells	Biomass	Cells	Biomass	Cells	Biomass	Cells	Biomass	Cells	Biomass
Minimum	3.1×10^4	1.1	20	0.01	40	0.01	2.6×10^4	0.07	194	0.1	40	0.06
Maximum	10.5×10^6	1686.8	6.4×10^6	97.5	1.4×10^6	327	3.7×10^6	9.7	8.5×10^5	357	9.6×10^6	1640
Average	11.2×10^5	106.9	2.5×10^5	3.8	5.3×10^4	11.4	4.6×10^5	1.2	9.5×10^4	44.7	2.7×10^5	46.4

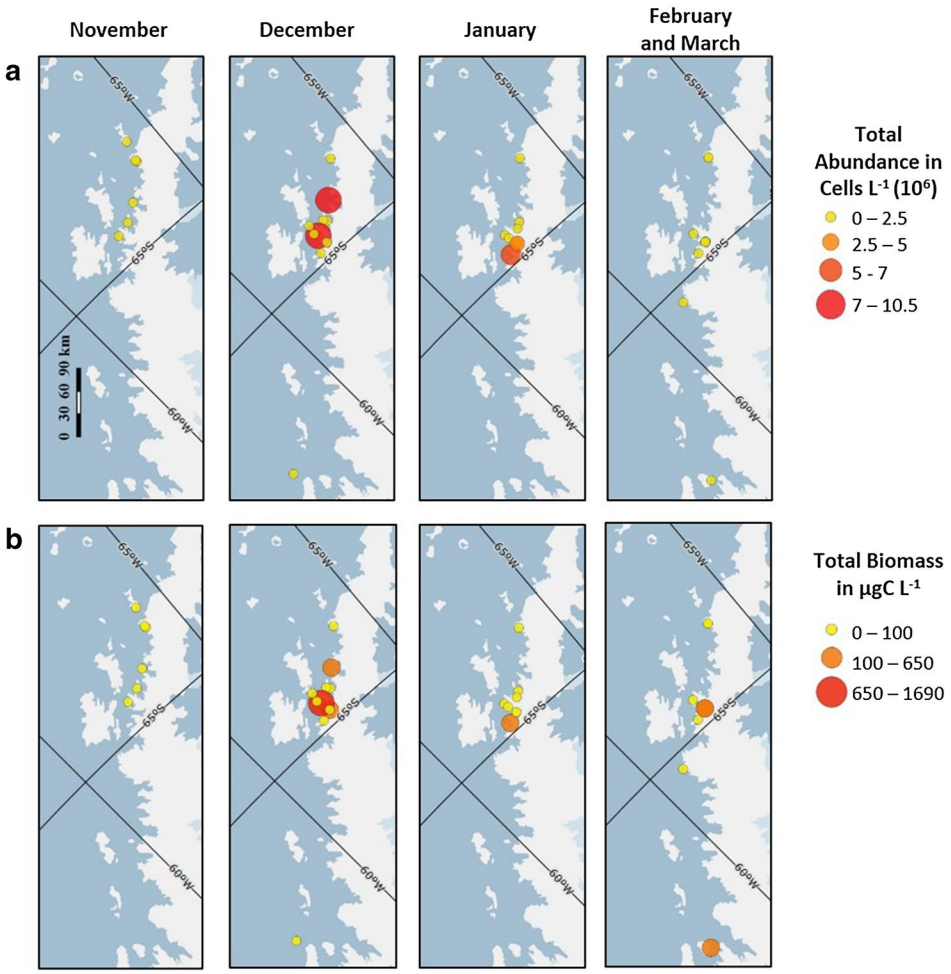

Fig. 2 Total phytoplankton abundance (**a**) and biomass (**b**) distribution by months during 2016–2017. Values of abundance and biomass are denoted by the size and color (yellow-orange-red) of the circles, with the references at the right for each case. (Color figure online)

sampling area (i.e., Hanusse Bay, sample 34), a peak of diatom biomass (273 µgC L^{-1}) was found, a similar assemblage with high abundances (1.2×10^5 cells L^{-1}) of *O. weissflogii* was present. To a lesser extent, other large-size diatom taxa such as *Proboscia* cf. *truncata* and *Corethron pennatum* significantly contributed to carbon biomass during December in all areas, and large organisms belonging to the genus *Coscinodiscus* (≥ 80 µm) were more important during the end of December and February in samples with high biomass. By contrast, diatom assemblages dominated by small diatoms (≤ 25 µm) such as *Chaetoceros* spp., *Fragilariopsis* spp., and *Thalassiosirales* ≤ 15 µm reached high abundances (e.g., sample 26, Table 2), but contributed less to biomass (~ 70 µgC L^{-1}) (Fig. 3).

Cryptophytes were observed in 93% of the samples, made great contributions to total phytoplankton abundance, mainly between the end of November and first days of January, when they reached up to ~ 75% of total phytoplankton (Fig. 3b). The highest cryptophyte abundance and biomass was found in December to mid-January, with a peak in December (Table 2, Fig. 3). By contrast, their relative abundance decreased in late summer. Cryptophyte specimens observed throughout this study presented a similar size and shape at OM, but they could not be identified to species (see following section).

Prasinophyceans were present in 80% of the samples but were usually a minor component of phytoplankton assemblages (Table 2), with the exception of a peak during a *Pyramimonas* sp. bloom in Neko Harbor in March 2016 (see following section). Although these organisms were also present in 2017, they reached lower concentrations (maximum of 3.4×10^5 cells L^{-1} and 77.5 µgC L^{-1} in sample 24). Two markedly different morphological types of prasinophyceans were identified during this study according to their cell length, small unidentified prasinophyceans (5–8 µm) and large cells belonging to the genus *Pyramimonas* (≥ 15 µm). Although, large *Pyramimonas* made contributions of up to 30–50% of the total biomass in some northern areas, i.e., Danco Island, Neko Harbor, and Paradise Harbor (samples 24, 25, 29, 30, and 41, Table 1), these organisms were not observed during this study in the three southernmost stations, south of 65°S.

Small unidentified flagellates (≤ 5 µm) were present in the entire studied period and usually dominated

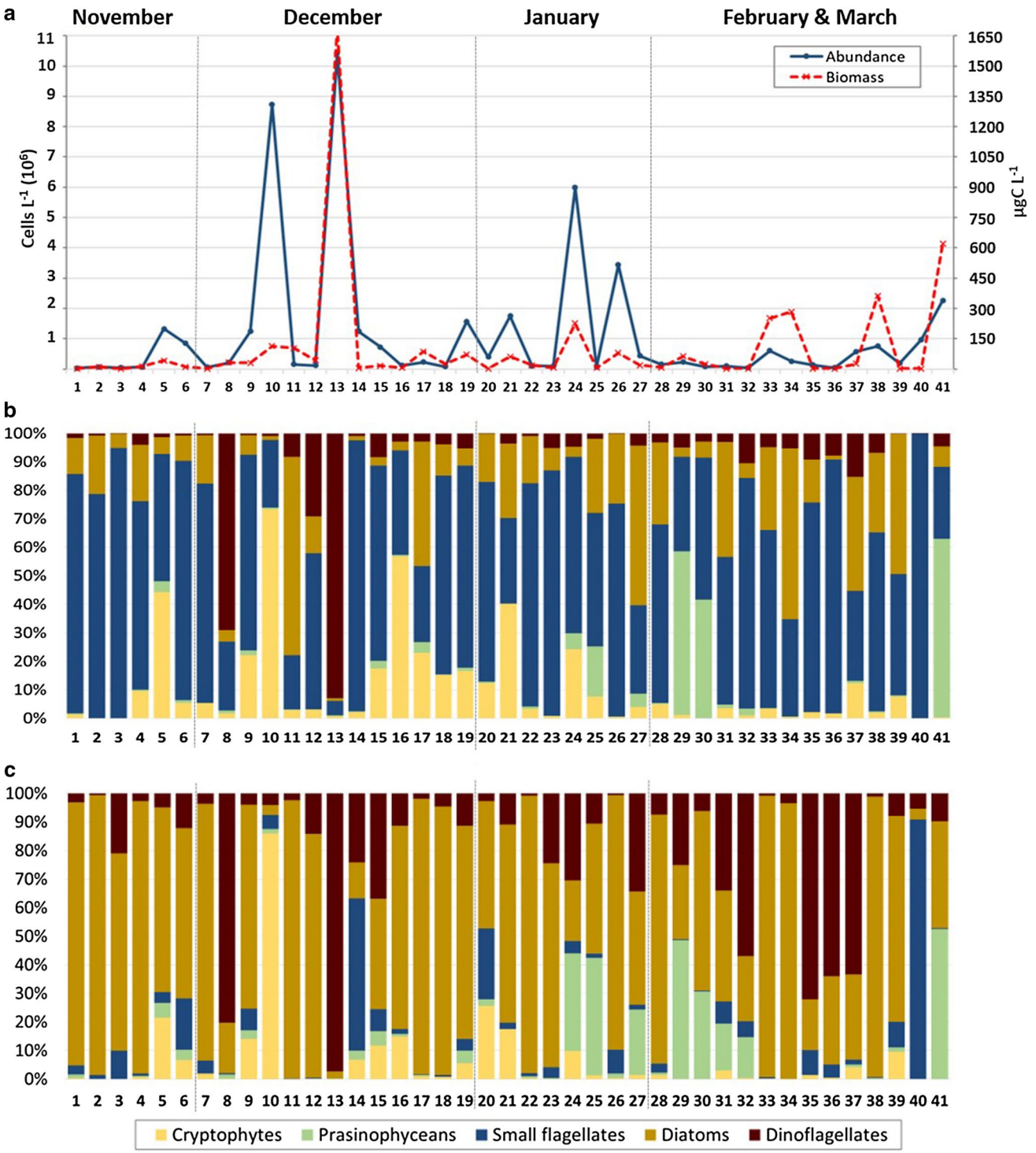

Fig. 3 **a** Total phytoplankton abundance and biomass distribution during 2016–2017. **b** Relative contribution of the five groups of phytoplankton to total cell abundance. **c** Relative contribution of the five groups of phytoplankton to total carbon biomass. 1—41 refer to sample number in Table 1. Samples 33, 38, 41 are ordered according to the month regardless of the year and therefore are anachronistic

phytoplankton abundance over the sampling season, reaching up to 90% of total phytoplankton cells in some samples, mainly during November (Fig. 3b). They were found in high abundance but represented very low biomass (Table 2).

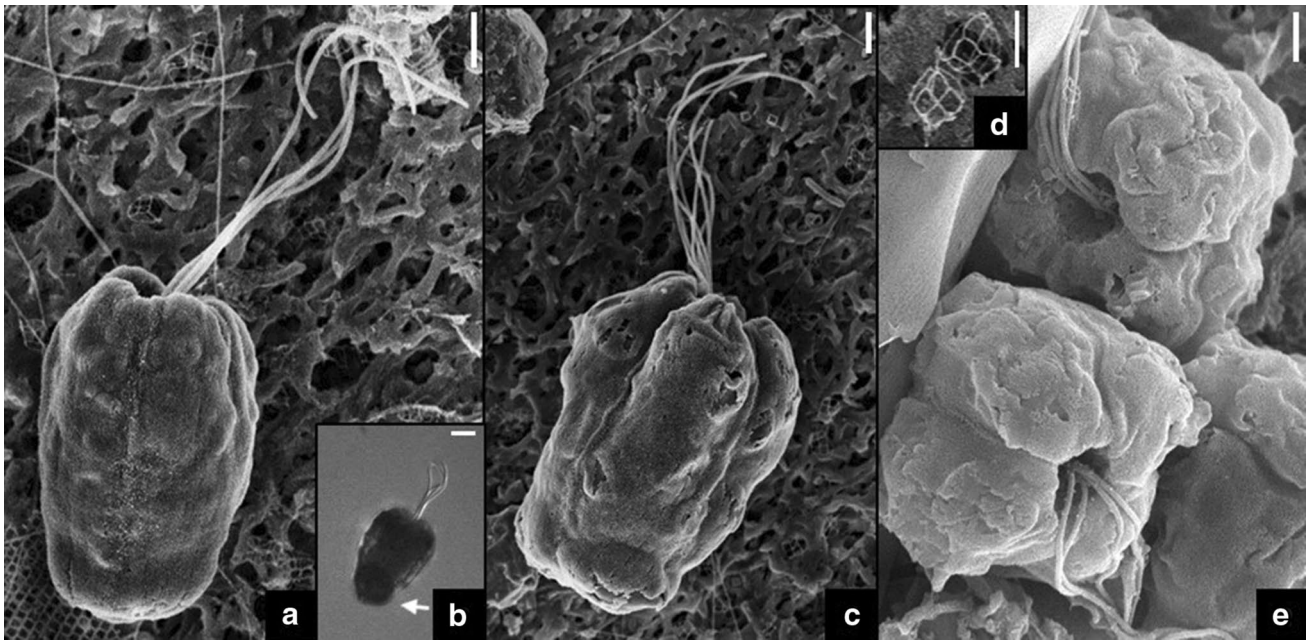

Fig. 4 *Pyramimonas* sp. Scale bars: 5 µm figure **b**; 2 µm figures **a**, **c** and **e**; 1 µm figure **d**. **a** SEM Large *Pyramimonas* quadriflagellated cell. **b** OM Large *Pyramimonas* quadriflagellated cell, with white arrow indicating the big pyrenoid. **c** SEM Large *Pyramimonas* octoflagellated cell, observe shape and size is similar to a quadriflagellated cell. **d** SEM observed unattached crown scales. **e** two large *Pyramimonas* in apical view showing the four rounded lobes and the apical depression

Main bloom-forming taxa

Three major peaks of phytoplankton abundance ($\geq 1.5 \times 10^6$ cells L^{-1} and ≥ 97.5 µgC L^{-1}) were observed during the time-lapse sampled. The morphology of the observed organisms that form these blooms is described chronologically below, supplemented with the details of location and magnitude of the blooms.

Pyramimonas sp. bloom

Based on microscopic observations of their morphology, the organisms in the *Pyramimonas* sp. bloom had a variable cell shape from oval to pyramidal (Fig. 4a–c), distinctly longer (19.2 ± 2.8 µm) than wide (12.9 ± 1.9 µm) (mean ± SD of 29 individuals). The apical end of the cell had four rounded lobes (Fig. 4c, e), while the antapical end was conical and rounded. Four or eight flagella, slightly longer than the body, emerged from an apical depression (Fig. 4a–c, e). A large pyrenoid was positioned centrally in the antapical end of the cell (Fig. 4b). Crown scales were observed unattached to the organisms in the material under SEM (Fig. 4d).

A bloom of these large *Pyramimonas* sp. cells was observed on March 3rd, 2016 in Neko Harbor (sample 41, Fig. 4), with 1.4×10^6 cells L^{-1} and 327 µgC L^{-1}, that represented 55% and 51% of total phytoplankton abundance and biomass, respectively.

Cryptophyte bloom

Microscopic observations of the cryptophyte cells in the bloom showed organisms with teardrop shape, with a very conical tail (Fig. 5a–c). Cells were 11.7 ± 1 µm in length and 5 ± 0.3 µm in width (mean ± SD of 20 individuals). The two flagella were slightly shorter than the body, emerging from an evident ventral furrow that was displaced to one side (Fig. 5a–c). The periplast was composed of small hexagonal to rectangular plates, the tail had no plates, with a warty appearance and an evident ventral band (Fig. 5a, c).

A bloom of these cryptophytes was observed on December 14th, 2016 at Wilhelmina Bay (sample 10, Table 2, Fig. 5). They represented around 73% of the total phytoplankton abundance and 85% of the total biomass in this sample.

Dinoflagellate bloom

Upon microscopic observation, the cells in this dinoflagellate bloom were unarmored and had variable shape, from rounded to slightly hexagonal in outline and slightly dorsoventrally flattened 12.6 ± 1.3 µm in width (mean ± SD of 20 individuals). The epicone was conical to round, the hypocone was hemispherical without a clear division, and larger than the epicone (Fig. 6b–c). The cingulum was

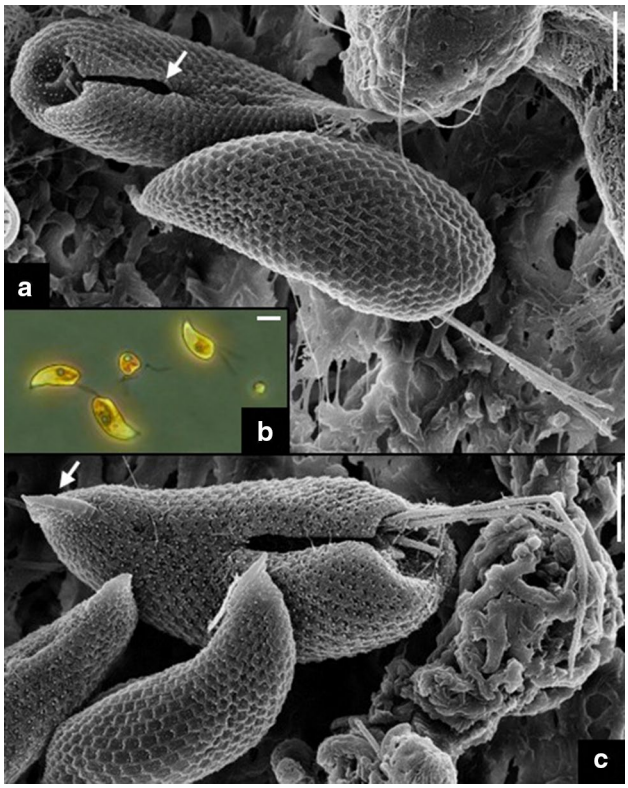

Fig. 5 Cryptophytes. Scale bars: 5 µm figure **b**; 2 µm figures **a** and **c. a** SEM two cryptophytes, one in ventral and one in dorsal view, observe teardrop shape, flagella, and periplast plates, white arrow indicating ventral furrow. **b** OM cryptophytes observe teardrop shape and flagella. **c** SEM cryptophytes, the central one in ventral view, white arrow indicating the ventral band of the tail, white arrowhead indicating insertion place of the two flagella

slightly displaced (Fig. 6b–c). The apical groove could not be observed under OM or SEM.

A bloom of these small naked dinoflagellates with an abundance of 9.5×10^6 cells L^{-1} and a biomass of 1597 µgC L^{-1} was observed on December 18th of 2016 at the Errera Channel, near Danco Island (sample 13, Fig. 6). In this sample, these organisms represented around 90% of the total phytoplankton abundance and 97% of the total biomass.

Discussion

Phytoplankton composition

The peaks of biomass and abundance found during this study along the WAP are comparable in magnitude to those previously reported for Bransfield and Gerlache Straits, Anvers Island (Palmer Station, 64°48′S–64°60′W) and Marguerite Bay (see Table 3). The highest phytoplankton abundance and biomass were observed during December and January 2016 and 2017 around the Danco coast (Fig. 2), coincident with a previously reported high benthic megafaunal congregation zone (Grange and Smith 2013). In order to compare values with previous studies that measured Chl-*a* in the WAP, we estimated a maximum of ~ 27.5 µg Chl-*a* L^{-1}—using the Carbon to Chl-*a* ratio provided by Montagnes et al. (1994)—associated with an unarmored dinoflagellate bloom (sample 13). This concentration is comparable to a large diatom and prymnesiophyte (*Phaeocystis pouchetii*) bloom previously observed by Holm-Hansen et al. (1989) in Gerlache Strait near Anvers Island (Table 3). Similar high Chl-*a* values in the Bransfield and Gerlache Straits have been related to other taxa besides diatoms and prymnesiophytes, such as prasinophyceans of the genus *Pyramimonas* (Table 3), but never to dinoflagellates. Rodriguez et al. (2002) attributed the recurrent spring and summer blooms of phytoflagellates, cryptophytes, and occasionally *Pyramimonas* in the Gerlache and Bransfield Straits to the interaction of different oceanographic processes, principally, the upper mixed layer stabilization by ice melting and the development of

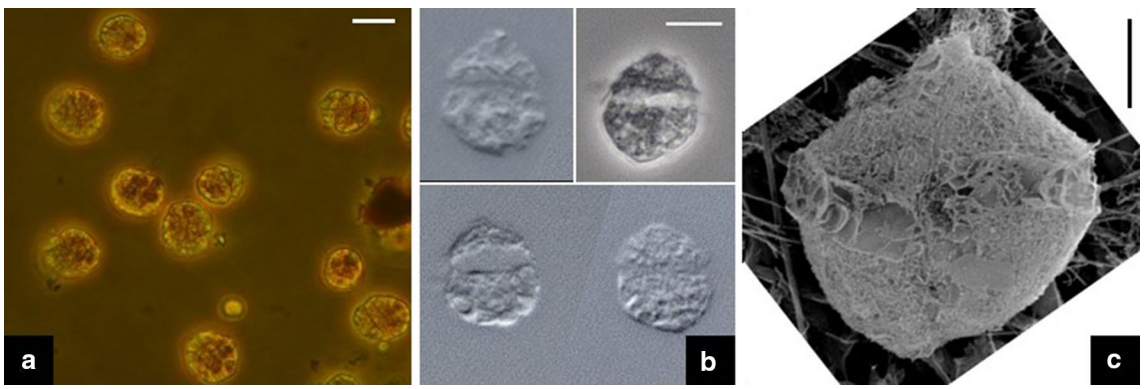

Fig. 6 Unarmored dinoflagellate. Scale bars: 10 µm figure **a**; 5 µm figure **b**; 2 µm figure **c**. **a** OM unarmored dinoflagellates bloom (200 ×). **b** OM unarmored dinoflagellates, notice shape diversity and size. **c** SEM unarmored dinoflagellate in ventral view, observe shape and the cingulum slightly displaced

Table 3 Comparison between the main phytoplankton blooms recorded in the WAP between Bransfield Strait and Marguerite Bay (between 63° and 68°S) and the blooms documented in this study

Taxa	Date	Area	Abundance (cells L^{-1})	Chl-*a* (μg L^{-1})/ Biomass (μgC L^{-1})	References
Pyramimonas sp.	January 1987	Gerlache Strait	$>7\times10^5$	25 μg L^{-1}	Bird and Karl (1991)
Diatoms (*Rhizosolenia* and *Odontella* spp.) + *Phaeocystis*	January 1987	Gerlache Strait	n/d	15–25 μg L^{-1}	Holm-Hansen et al. (1989)
Cryptophytes (*Cryptomonas* cf. *acuta*)	December 1991/January 1992	Gerlache Strait	3×10^6	15.4 μg L^{-1}	Ferrario and Sar (1992)
Cryptophytes	December 1991/January 1992	Gerlache Strait	n/d	< 10 μg L^{-1}	Vernet (1992)
Crytophytes (*Cryptomonas* sp.)	December 1995	Bransfield Strait	6.36×10^6	n/d	Rodriguez et al. (2002)
P. gelidicola	January 1996	Gerlache Strait	1.73×10^6	n/d	Rodriguez et al. (2002)
Cryptophytes	January 1996	Anvers Island	11.3×10^6	229 μgC L^{-1}	Garibotti et al. (2005)
Diatoms (mainly *E. antarctica, O. weissflogii* and *Coscinodiscus bouvet*) + *Phaeocystis*	February 1996	Marguerite Bay	2.1×10^6	1563 μgC L^{-1}	Garibotti et al. (2005)
Diatoms (mainly *E. antarctica, O. weissflogii*) + *Phaeocystis*	February 1997	Marguerite Bay	4.2×10^6	888 μgC L^{-1}	Garibotti et al. (2005)
Cryptophytes	January 1999	Anvers Island	15.7×10^6	369 μgC L^{-1}	Garibotti et al. (2005)
Diatoms (mainly *C. bouvet* and *Chaetoceros socialis*) + *Phaeocystis*	February 1999	Marguerite Bay	6×10^6	1442 μgC L^{-1}	Garibotti et al. (2005)
Cryptophytes	January 2010	Bransfield Strait	5×10^5	30.7–38.2 μgC L^{-1}	García-Muñoz et al. (2013)
Cryptophytes	February 2010	Bransfield Strait	n/d	16.9 μgC L^{-1}	Mendes et al. (2013)
Diatoms (*Thalassiosira* spp., *Chaetoceros* spp.)	February 2017	Southern Bay	n/d	19.7 μg L^{-1}	Höfer et al. (2019)
Pyramimonas sp.	March 2016	Neko Harbor	1.4×10^6	327 μgC L^{-1}	This study
Cryptophytes	December 2016	Wilhelmina Bay	6.4×10^6	97.5 μgC L^{-1}	This study
Unarmored dinoflagellates	December 2016	Danco Island	9.5×10^6	1597 μgC L^{-1}	This study

n/d for no data

frontal systems. We expect similar processes in our sampling area, mainly from nearby glacier fronts delivering freshwater (Dierssen et al. 2002; Meredith et al. 2008).

In spite of the large variability in the abundance and biomass of the main phytoplankton groups (Fig. 3), general patterns of temporal distribution can be observed. December and January presented the highest cryptophyte cell abundance (Fig. 3b), similar to the observations by Schofield et al. (2017) who studied phytoplankton taxa by pigments in the vicinity of Anvers Island. However, because of their small size, cryptophytes usually did not dominate the phytoplankton biomass (Fig. 3c). Prasinophyceans were important biomass contributors, later in the season, from the end of January to March (Fig. 3c), coexisting with large diatoms. The main components of this group were organisms belonging to the genus *Pyramimonas*. Prasinophyceans are known to be a common component of the summer phytoplankton in the WAP, sometimes developing blooms (Rodriguez et al. 2002; Garibotti et al. 2003a, 2005; Schofield et al. 2017). In these nearshore waters at the time of sampling, we did not observe a conspicuous diatom spring bloom during November or December, as described for the WAP continental shelf and south of Anvers Island after sea ice retreat (Garibotti et al. 2005; Kim et al. 2016). Our results suggest that the diatom spring bloom may not develop in these nearshore waters. However, with only one year of sampling it is not possible to generalize. Low sea ice cover in the fjords and passages in 2016 may have caused a delay in water-column stratification and prevented the formation of the classic diatom bloom, as explained by Rozema et al. (2017) for Marguerite Bay.

The nanoplanktonic fraction (2–20 μm) predominated numerically over the microplankton (> 20 μm) during this study. Small unidentified flagellates and cryptophytes were the most abundant groups sampled (Fig. 3b). In addition, the three main peaks in abundance (i.e., blooms) were composed by nanoflagellated-size taxa. Nanophytoplankton abundance was usually dominated by small (≤ 5 μm) unidentified cells (Fig. 3b), which resembled single cells of *Phaeocystis* sp. (prymnesiophytes). The occurrence of the typical spherical colonies (Zingone et al. 2011) was not detected. Single-cell *Phaeocystis* is the dominant form in WAP shelf waters,

with the exception of Marguerite Bay where the colonial *Phaeocystis* sp. is associated with diatoms (Garibotti et al. 2003a; Rozema et al. 2017). Similarly, the colonial form of *Phaeocystis antarctica*, usually associated with diatoms, is a recurrent phytoplankton component in the Bransfield and Gerlache Straits (Rodriguez et al. 2002). Therefore, the spring–summer phytoplankton community in the study area, when influenced by glacier discharge (Pan et al. 2019), seems to be dominated by flagellates, similar to previous observations in austral summer in the WAP, based on chlorophyll size fraction and microscopy (Holm-Hansen et al. 1989; Rodriguez et al. 2002; Garibotti et al. 2003a).

The absence of a bloom of large diatoms was unexpected as diatoms are considered a key component in Antarctica, well-known to be found in high concentration in the summer months in the WAP continental shelf and further south, in Marguerite Bay, associated with the sea ice edge (Table 3). Although, in our study, diatoms were important biomass producers during the sampled season (Fig. 3b), they did not reach previously reported high values (e.g., up to 1563 µgC L^{-1}, Table 3). In our study area in 2016–2017 diatom biomass did not reach values higher than 357 µgC L^{-1}, coinciding with summers of low diatom abundance (Garibotti et al. 2005). Similar to WAP shelf waters, the diatom *O. weissflogii* contributed significantly to biomass in February–March 2016 as well as during January–February 2017.

A predominance of cryptophytes has been documented in the last decades in the WAP shelf waters (Moline et al. 2004; Montes-Hugo et al. 2009). In the Bransfield Strait, cryptophyte populations seem to be increasing as well, and the question of what factors benefit these organisms is still unanswered (Mendes et al. 2013, 2018). In the same way, in this study, cryptophytes were a conspicuous component of the phytoplankton community (Fig. 3b). Cryptophyte dominance have been previously attributed to, among other reasons, selective grazing and the stability of the upper mixed layer (Garibotti et al. 2003a), and to preference/physiological tolerance of these organisms to lower salinity (Moline et al. 2004). Likewise, Mendes et al. (2018) recently hypothesized that cryptophytes would have photophysiological plasticity to tolerate high irradiances in the upper layers and bloom under such conditions. Although our study does not allow us to make inferences about the factors that could benefit cryptophytes, it does suggest for 2016–2017 a greater importance of nanoflagellates, such as cryptophytes, over microplanktonic diatoms, in these nearshore waters of the WAP.

Dinoflagellates were the principal biomass contributors, reaching the highest abundance and biomass values in December. Within this group, small unarmored dinoflagellates dominated over large armored genera, similar to previous studies in WAP shelf waters (Garibotti et al. 2003b; Garzio and Steinberg 2013). Unarmored dinoflagellates have never been found in high abundance in the WAP (Rodriguez et al. 2002; Garibotti et al. 2003a, b; Garzio and Steinberg 2013; Gonçalves-Araujo et al. 2015; Arrigo et al. 2017; Schofield et al. 2017). Maximum registered values of dinoflagellate abundance in the Gerlache Strait do not exceed 4×10^5 cells L^{-1} (Rodriguez et al. 2002) and 18–20 µgC L^{-1} in shelf waters of the WAP (Garibotti et al. 2003a; Garzio and Steinberg 2013). The dinoflagellate bloom observed in our study was thus 20-80 fold higher (Table 2) than previous records in this region. Despite blooms of the small dinoflagellate *Polarella glacialis* (up to 4×10^6 cells L^{-1}) related to fast sea ice during November and December in East Antarctica, i.e., McMurdo Sound (Stoecker et al. 1992; Montresor et al. 1999) and Davis Station (Thomson et al. 2006), our findings represent the first dinoflagellate bloom of this magnitude reported for the WAP.

This study represents the first attempt to a comprehensive description of the phytoplankton community in unexplored WAP nearshore waters, possible by cooperation with IAATO ships through FjordPhyto, a Citizen Science project. Citizen Science involvement in ecological studies is becoming a mainstay of research aimed at biodiversity monitoring and conservation (Dickinson et al. 2010; Chandler et al. 2017; McKinley et al. 2017). Future sampling efforts in the frame of this project will include the collection of environmental and metagenomic data to refine and complete phytoplankton dynamics and species diversity described in this study.

Identification of the main bloom-forming taxa

Pyramimonas sp. (Prasinophyceae)

There are three species of *Pyramimonas* described for Antarctica, two species with small cells *P. australis* (8–10 µm long and 5–6 µm wide) and *P. tychotreta* (8–12 µm long and 6–8 µm wide), and *P. gelidicola*, with larger cells (14–18 µm long and 8–9 µm wide) (McFadden et al. 1982; Daugbjerg 2000; Moro et al. 2002). Although size is not enough for species delimitation, the large *Pyramimonas* cells observed during this study (15–23 µm long and 10–17.5 µm wide) had closer dimensions to *P. gelidicola*. The identification at species level of *Pyramimonas* is mainly based on the morphology of the scales that cover their body (Norris and Pienaar 1978; McFadden et al. 1986; Hori et al. 1995; Alonso-González et al. 2014), based on transmission electron microscopy (TEM) observations. Unfortunately, only a few crown scales were observed during our SEM observations, which were not enough for species identification. In addition, we observed several cells with eight flagella, which do not coincide with the quadriflagellated cells previously described for *P. gelidicola* (McFadden et al. 1982). The possibility that these octoflagellated cells may present a division stage is also considered; however, these octoflagellated cells had the same morphology and size as quadriflagellate cells

and were quite abundant. There are other species of *Pyramimonas* such as *P. amylifera* that presents quadriflagellated and octoflagellated vegetative cells (Hargraves and Gardiner 1980) suggesting we could have observed only one species with either 4 or 8 flagella.

The occurrence of *Pyramimonas* blooms in this region has been previously described for the northern Gerlache Strait (Table 3). Bird and Karl (1991) remarked that the organisms they observed were bigger than *P. gelidicola*, in coincidence with our observations, but they only observed quadriflagellated cells. Rodriguez et al. (2002) recorded another bloom years later of large-sized *Pyramimonas* that they concluded might be *P. gelidicola* from their pigment pattern.

Cryptophytes

The morphology of the cryptophyte blooming organisms does not resemble *Geminigera cryophila*, the only cryptophyte species described from Antarctica (Taylor and Lee 1971; Hill 1991). *G. cryophila* has a rounded shape and a characteristic warty aspect because of the prolific accumulation of lipid droplets in the peripheral cytoplasm (Taylor and Lee 1971). By contrast, the cells observed in this study presented a teardrop morphology and lack the lipid droplets. Ferrario and Sar (1992) reported the occurrence of *Cryptomonas* cf. *acuta* (now *Teleaulax acuta*) in the Gerlache Strait (Table 3), which presented the similar teardrop morphology than the individuals we found. However, these authors did not provide comments about the cellular fine morphology or the justification for their identification. Our detailed morphological analysis showed organisms with a teardrop cell shape, hexagonal periplast plates covering the body excepting the tail, evident furrow, and a mid-ventral band in the tail (Fig. 5). Despite the teardrop cell shape resembling *Teleaulax acuta*, this species has a featureless periplast and a more extended furrow, whereas it lacks the distinguished tail with a central band (Hill 1991; Laza-Martínez et al. 2012). By contrast, these organisms seem to be very similar to the unidentified cryptophyte that Scott and Marchant (2005) and van den Hoff and Bell (2015) found in East Antarctica. The previously described characteristics of the blooming cryptophytes make us believe that they could be related to the genus *Plagioselmis* (Brett et al. 1994; Clay et al. 1999; Novarino 2003), although these characteristics, principally the size and shape of the hexagonal periplast plates, do not coincide with any currently described species (Novarino 2003, 2005).

There are several previous records of cryptophyte blooms in the Gerlache and Bransfield Straits, also in coastal WAP and shelf waters (see Table 3). However, only Garibotti et al. (2005) and Rodriguez et al. (2002) record higher abundances than those registered in the nearshore waters analyzed in this study (Table 3). In this way, our data suggest this region supports large cryptophyte blooms composed possibly of a new species.

Unarmored dinoflagellates

The unarmored dinoflagellates are an understudied group. Their fragility makes them difficult to identify under OM and find diagnostic characters for their classification (Gómez et al. 2011). There are a few early drawings and descriptions of unarmored dinoflagellates taxa in Antarctic waters based on the morphology of the cell observed under OM, (i.e., Balech 1958, 1976; Yoshine 1970). These descriptions are no longer valid since modern classification methods combine molecular and fine morphology under SEM (Daugbjerg 2000). However, a few more recent studies have combined morphology and molecular analysis to successfully describe new small unarmored dinoflagellates in Antarctica (e.g., Montresor et al. 1999; De Salas et al. 2008). Nowadays a large number of gene sequences have been found in Antarctic waters that approach dinoflagellate DNA but they have not yet been assigned to a particular taxon (López-García et al. 2001; Luo et al. 2016).

The shape of the apical groove is remarkably important for the morphological identification of unarmored dinoflagellates (Daugbjerg et al. 2000). The inability to observe the apical groove in our specimens (Fig. 6), that could be related to cell fixation or deterioration (Haywood et al. 2004), does not allow us to make inferences about their identity, despite numerous attempts under OM and SEM. However, the cell shape and size of the observed dinoflagellates resemble some Antarctic species of *Karlodinium* and *Takayama* (De Salas et al. 2008). Even though these descriptions come from East Antarctica, molecular studies from Potter Cove and Fildes Bay in King George Island have found sequences close to these two genera (Luo et al. 2016; Abele et al. 2017), suggesting that these dinoflagellates may also be present in this region. Gast et al. (2006, 2007) also reported a *Karenia*- or *Karlodinium*-related species as a dominant unarmored dinoflagellate in the Ross Sea, Antarctica, although they did not formally describe the taxon. However, these organisms did not resemble our observations, they were larger than the ones we found and their cell morphology was different. It is important to combine molecular and morphological approaches in the nearshore waters of the WAP in order to obtain a definitive answer on the unarmored dinoflagellates that are found in these waters.

Conclusions

This study supports the notion that nearshore waters of the WAP are an important region for phytoplankton biomass accumulation, and provides a first characterization of the phytoplankton composition over a large geospatial and temporal scale in these relatively unexplored coastal areas. This region between 63° and 67°S comprises fjords with tidewater glaciers, passages, and straits in between islands. These locations sampled are visited throughout the austral spring and summer by tourist vessels. The sampling efforts achieved through the Citizen Science platform with Antarctic tour operators allowed a continuous and extensive view of the phytoplankton community composition and distribution along a latitudinal and temporal gradient. The phytoplankton composition of this region, in the sampled period, seems to be different from the better-described WAP shelf waters and Bransfield Strait: few large bloom-forming diatom species were observed from November to March and none of them were numerically abundant. Our results highlight the importance of nanophytoflagellates (unidentified phytoflagellates, cryptophytes, prasinophyceans, prymnesiophytes and small unarmored dinoflagellates) in the nearshore waters of the WAP. The observed blooms of cryptophytes and prasinophyceans coincide with previous observations in slope and shelf waters in this region. Furthermore, we detected a large bloom of small unarmored dinoflagellates, the first documented in the WAP. Detailed microscopic observations were not enough for the specific identification of the three main blooming organisms, and some of them seem to not coincide with similar organisms previously described for Antarctica. Combined molecular and further morphological analyses are needed to determine their specific identity.

Acknowledgements This study was supported by Grant PIP 0122 from Consejo Nacional de Investigaciones Científicas y Técnicas (CONICET, Argentina) to G.O.A, a doctoral fellowship from CONICET to M.M., and a U.S. National Science Foundation (NSF) Public Participation in STEM (Science, Technology, Engineering, Math) Research (PPSR) award PLR-1443705 to M.V. We would especially like to thank our partners with the International Association of Antarctica Tour Operators (IAATO), the participating passengers, the crew, and the science personnel on board Antarctic cruises MS Expedition operated by G Adventures and MS Hebridean Sky operated by Polar Latitudes for providing shiptime and samples in support of this research project during the 2016–2017 season. We also thank the reviewers for the comments, the manuscript has improved substantially.

Compliance with ethical standards

Conflict of interest The authors declare that they do not have any conflicts of interest with the data presented in this scientific article.

References

Abele D, Vazquez S, Buma AGJ et al (2017) Pelagic and benthic communities of the Antarctic ecosystem of Potter Cove: genomics and ecological implications. Mar Genomics 33:1–11. https://doi.org/10.1016/j.margen.2017.05.001

Alonso-González A, Orive E, David H et al (2014) Scaly green flagellates from Spanish Atlantic coastal waters: molecular, ultrastructural and pigment analyses. Bot Mar 57:379–402. https://doi.org/10.1515/bot-2013-0108

Arrigo KR, van Dijken GL, Alderkamp A-C et al (2017) Early spring phytoplankton dynamics in the Western Antarctic Peninsula. J Geophys Res Ocean 122:9350–9369. https://doi.org/10.1002/2017JC013281

Balech E (1958) Plancton de la Campaña Antártica Argentina 1954-1955. Physis 21:75–108

Balech E (1976) Clave ilustrada de dinoflagelados antárticos. Publ Inst Antart Argent 11:1–79

Bird DF, Karl DM (1991) Massive prasinophyte bloom in northern Gerlache Strait. Antarct J US 26:152–154

Brett SJ, Perasso L, Wetherbee R (1994) Structure and development of the cryptomonad periplast: a review. Protoplasma 181:106–122. https://doi.org/10.1007/BF01666391

Chandler M, See L, Copas K et al (2017) Contribution of citizen science towards international biodiversity monitoring. Biol Conserv 213:280–294. https://doi.org/10.1016/j.biocon.2016.09.004

Clay BL, Kugrens P, Lee RE (1999) A revised classification of Cryptophyta. Bot J Linn Soc 131:131–151. https://doi.org/10.1111/j.1095-8339.1999.tb01845.x

Cook AJ, Holland PR, Meredith MP et al (2016) Ocean forcing of glacier retreat in the western Antarctic Peninsula. Science 353:283–286. https://doi.org/10.1126/science.aae0017

Daugbjerg N (2000) *Pyramimonas tychotreta*, sp. nov. (Prasinophyceae), a new marine species from Antarctica: light and electron microscopy of the motile stage and notes on growth rates. J Phycol 36:160–171. https://doi.org/10.1046/j.1529-8817.2000.99157.x

Daugbjerg N, Hansen G, Larsen J, Moestrup Ø (2000) Phylogeny of some of the major genera of dinoflagellates based on ultrastructure and partial LSU rDNA sequence data, including the erection of three new genera of unarmoured dinoflagellates. Phycologia 39:302–317

De Salas MF, Laza-Martínez A, Hallegraeff GM (2008) Novel unarmored dinoflagellates from the toxigenic family Kareniaceae (Gymnodiniales): five new species of *Karlodinium* and one new *Takayama* from the Australian sector of the Southern Ocean. J Phycol 44:241–257. https://doi.org/10.1111/j.1529-8817.2007.00458.x

Dickinson JL, Zuckerberg B, Bonter DN (2010) Citizen science as an ecological research tool: challenges and benefits. Annu Rev Ecol Evol Syst 41:149–172. https://doi.org/10.1146/annurev-ecolsys-102209-144636

Dierssen HM, Smith RC, Vernet M (2002) Glacial meltwater dynamics in coastal waters west of the Antarctic peninsula. Proc Natl Acad Sci 99:1790–1795. https://doi.org/10.1073/pnas.032206999

Ducklow H, Fraser W, Meredith M et al (2013) West Antarctic Peninsula: an ice-dependent coastal marine ecosystem in transition. Oceanography 26:190–203. https://doi.org/10.5670/oceanog.2013.62

Edler L, Elbrächter M (2010) The Utermöhl method for quantitative phytoplankton analysis. Microsc Mol Methods Quant Phytoplankton Anal 110:13–20

Ferrario M, Sar E (1992) RACER: phytoplankton populations in the Gerlache Strait. Antarct J US 27:158–159

Ferrario ME, Sar EA, Vernet M (1998) *Chaetoceros* resting spores in the Gerlache Strait, Antarctic Peninsula. Polar Biol 19:286–288. https://doi.org/10.1007/s003000050247

García-Muñoz C, Lubián LM, García CM et al (2013) A mesoscale study of phytoplankton assemblages around the South Shetland Islands (Antarctica). Polar Biol 36:1107–1123. https://doi.org/10.1007/s00300-013-1333-5

Garibotti I, Vernet M, Ferrario M et al (2003a) Phytoplankton spatial distribution patterns along the western Antarctic Peninsula (Southern Ocean). Mar Ecol Prog Ser 261:21–39. https://doi.org/10.3354/meps261021

Garibotti I, Vernet M, Kozlowski W, Ferrario M (2003b) Composition and biomass of phytoplankton assemblages in coastal Antarctic waters: a comparison of chemotaxonomic and microscopic analyses. Mar Ecol Prog Ser 247:27–42. https://doi.org/10.3354/meps247027

Garibotti IA, Vernet M, Ferrario ME (2005) Annually recurrent phytoplanktonic assemblages during summer in the seasonal ice zone west of the Antarctic Peninsula (Southern Ocean). Deep Sea Res Part I Oceanogr Res Pap 52:1823–1841. https://doi.org/10.1016/j.dsr.2005.05.003

Garzio LM, Steinberg DK (2013) Microzooplankton community composition along the Western Antarctic Peninsula. Deep Sea Res Part I Oceanogr Res Pap 77:36–49. https://doi.org/10.1016/j.dsr.2013.03.001

Gast RJ, Moran DM, Beaudoin DJ et al (2006) Abundance of a novel dinoflagellate phylotype in the Ross Sea, Antarctica. J Phycol 42:233–242. https://doi.org/10.1111/j.1529-8817.2006.00183.x

Gast RJ, Moran DM, Dennett MR, Caron DA (2007) Kleptoplasty in an Antarctic dinoflagellate: caught in evolutionary transition? Environ Microbiol 9:39–45. https://doi.org/10.1111/j.1462-2920.2006.01109.x

Gómez F, Moreira D, López-García P (2011) Advances on the study of dinoflagellates (Dinophyceae) with the molecular phylogeny. Hidrobiológica 21:343–364

Gonçalves-Araujo R, de Souza MS, Tavano VM, Garcia CAE (2015) Influence of oceanographic features on spatial and interannual variability of phytoplankton in the Bransfield Strait, Antarctica. J Mar Syst 142:1–15. https://doi.org/10.1016/j.jmarsys.2014.09.007

Grange LJ, Smith CR (2013) Megafaunal communities in rapidly warming Fjords along the West Antarctic Peninsula: hotspots of abundance and beta diversity. PLoS ONE 8:e77917. https://doi.org/10.1371/journal.pone.0077917

Hargraves PE, Gardiner WE (1980) The life history of *Pyramimonas amylifera* Conrad (Prasinophyceae). J Plankton Res 2:99–108. https://doi.org/10.1093/plankt/2.2.99

Haywood AJ, Steidinger KA, Truby EW et al (2004) Comparative morphology and molecular phylogenetic analysis of three new species of the genus *Karenia* (Dinophyceae) from New Zealand. J Phycol 40:165–179. https://doi.org/10.1046/j.1529-8817.2004.02149.x

Hill DRA (1991) A revised circumscription of *Cryptomonas* (Cryptophyceae) based on examination of Australian strains. Phycologia 30:170–188

Hillebrand H, Claus-Dieter D, Kirschtel D et al (1999) Biovolume calculation for pelagic and benthic microalgae. J Phycol 35:403–424

Höfer J, Giesecke R, Hopwood MJ et al (2019) The role of water column stability and wind mixing in the production/export dynamics of two bays in the Western Antarctic Peninsula. Prog Oceanogr. https://doi.org/10.1016/j.pocean.2019.01.005

Holm-Hansen O, Mitchell BG, Hewes CD, Karl DM (1989) Phytoplankton blooms in the vicinity of palmer station, Antarctica. Polar Biol 10:49–57. https://doi.org/10.1007/BF00238290

Hori T, Moestrup Ø, Hoffman LR (1995) Fine structural studies on an ultraplanktonic species of *Pyramimonas*, *P. virginica* (Prasinophyceae), with a discussion of subgenera within the genus *Pyramimonas*. Eur J Phycol 30:219–234. https://doi.org/10.1080/09670269500651001

Kim H, Doney SC, Iannuzzi RA et al (2016) Climate forcing for dynamics of dissolved inorganic nutrients at Palmer Station, Antarctica: an interdecadal (1993–2013) analysis. J Geophys Res Biogeosciences 121:2369–2389. https://doi.org/10.1002/2015JG003311

Laza-Martínez A, Arluzea J, Miguel I, Orive E (2012) Morphological and molecular characterization of *Teleaulax gracilis* sp. nov. and *T. minuta* sp. nov. (Cryptophyceae). Phycologia 51:649–661. https://doi.org/10.2216/11-044.1

López-García P, Rodríguez-Valera F, Pedrós-Alió C, Moreira D (2001) Unexpected diversity of small eukaryotes in deep-sea Antarctic plankton. Nature 409:603

Lund JWG, Kipling C, Le Cren ED (1958) The inverted microscope method of estimating algal numbers and the statistical basis of estimations by counting. Hydrobiologia 11:143–170. https://doi.org/10.1007/BF00007865

Luo W, Li H, Gao S et al (2016) Molecular diversity of microbial eukaryotes in sea water from Fildes Peninsula, King George Island, Antarctica. Polar Biol 39:605–616. https://doi.org/10.1007/s00300-015-1815-8

May SE, McClennen CE, Domack EW (1991) Diatom assemblages within surface waters of Andvord Bay, Antarctica. Antarct J US 26:112–115

McFadden GI, Moestrup Ø, Wetherbee R (1982) *Pyramimonas gelidicola* sp. nov. (Prasinophyceae), a new species isolated from Antarctic sea ice. Phycologia 21:103–111

McFadden GI, Hill DRA, Wetherbee R (1986) A study of the genus *Pyramimonas* (Prasinophyceae) from southeastern Australia. Nord J Bot 6:209–234. https://doi.org/10.1111/j.1756-1051.1986.tb00875.x

McKinley DC, Miller-Rushing AJ, Ballard HL et al (2017) Citizen science can improve conservation science, natural resource management, and environmental protection. Biol Conserv 208:15–28. https://doi.org/10.1016/j.biocon.2016.05.015

Menden-Deuer S, Lessard EJ (2000) Carbon to volume relationships for dinoflagellates, diatoms, and other protist plankton. Limnol Oceanogr 45:569–579. https://doi.org/10.4319/lo.2000.45.3.0569

Mendes CRB, Tavano VM, Leal MC et al (2013) Shifts in the dominance between diatoms and cryptophytes during three late summers in the Bransfield Strait (Antarctic Peninsula). Polar Biol 36:537–547. https://doi.org/10.1007/s00300-012-1282-4

Mendes CRB, Tavano VM, Dotto TS et al (2018) New insights on the dominance of cryptophytes in Antarctic coastal waters: a case study in Gerlache Strait. Deep Sea Res Part II Top Stud Oceanogr 149:161–170. https://doi.org/10.1016/j.dsr2.2017.02.010

Meredith MP, King JC (2005) Rapid climate change in the ocean west of the Antarctic Peninsula during the second half of the 20th century. Geophys Res Lett 32:1–5. https://doi.org/10.1029/2005GL024042

Meredith MP, Brandon MA, Wallace MI et al (2008) Variability in the freshwater balance of northern Marguerite Bay, Antarctic Peninsula: results from δ18O. Deep Res Part II Top Stud Oceanogr 55:309–322. https://doi.org/10.1016/j.dsr2.2007.11.005

Meredith MP, Stammerjohn SE, Venables HJ et al (2016) Changing distributions of sea ice melt and meteoric water west of the Antarctic Peninsula. Deep Sea Res Part II Top Stud Oceanogr 139:40–57. https://doi.org/10.1016/j.dsr2.2016.04.019

Moline MA, Claustre H, Frazer TK et al (2004) Alteration of the food web along the Antarctic Peninsula in response to a regional warming trend. Glob Chang Biol 10:1973–1980. https://doi.org/10.1111/j.1365-2486.2004.00825.x

Montagnes DJS, Berges JA, Harrison PJ, Taylor FJR (1994) Estimating carbon, nitrogen, protein, and chlorophyll a from volume in

marine phytoplankton. Limnol Oceanogr 39:1044–1060. https://doi.org/10.4319/lo.1994.39.5.1044
Montes-Hugo M, Doney SC, Ducklow HW et al (2009) Recent changes in phytoplankton communities associated with rapid regional climate change along the Western Antarctic peninsula. Science 323:1470–1473. https://doi.org/10.1126/science.1164533
Montresor M, Procaccini G, Stoecker DK (1999) *Polarella glacialis*, gen. nov., sp. nov.(Dinophyceae): Suessiaceae are still alive! J Phycol 35:186–197
Moro I, La Rocca N, Dalla Valle L et al (2002) *Pyramimonas australis* sp. nov. (Prasinophyceae, Chlorophyta) from Antarctica: fine structure and molecular phylogeny. Eur J Phycol 37:103–114. https://doi.org/10.1017/S0967026201003493
Norris RE, Pienaar RN (1978) Comparative fine-structural studies on five marine species of *Pyramimonas* (Chlorophyta, Prasinophyceae). Phycologia 17:41–51
Novarino G (2003) A companion to the identification of cryptomonad flagellates (Cryptophyceae = Cryptomonadea). Hydrobiologia 502:225–270
Novarino G (2005) Nanoplankton protists from the western Mediterranean Sea. II. Cryptomonads (Cryptophyceae = Cryptomonadea). Sci Mar 69:47–74. https://doi.org/10.3989/scimar.2005.69n147
Nowacek DP, Friedlaender AS, Halpin PN et al (2011) Super-aggregations of krill and humpback whales in Wilhelmina bay, Antarctic Peninsula. PLoS ONE 6:2–6. https://doi.org/10.1371/journal.pone.0019173
Pan JB, Vernet M, Reynolds RA, Mitchell GB (2019) The optical and biological properties of glacial meltwater in an Antarctic fjord. PLoS ONE 14:1–30. https://doi.org/10.1371/journal.pone.0211107
Rodriguez F, Varela M, Zapata M (2002) Phytoplankton assemblages in the Gerlache and Bransfield Straits (Antarctic Peninsula) determined by light microscopy and CHEMTAX analysis of HPLC pigment data. Deep Sea Res Part II Top Stud Oceanogr 49:723–747. https://doi.org/10.1016/S0967-0645(01)00121-7
Rozema PD, Venables HJ, van de Poll WH et al (2017) Interannual variability in phytoplankton biomass and species composition in northern Marguerite Bay (West Antarctic Peninsula) is governed by both winter sea ice cover and summer stratification. Limnol Oceanogr 62:235–252. https://doi.org/10.1002/lno.10391
Schloss IR, Wasilowska A, Dumont D et al (2014) On the phytoplankton bloom in coastal waters of southern King George Island (Antarctica) in January 2010: an exceptional feature? Limnol Oceanogr 59:195–210. https://doi.org/10.4319/lo.2014.59.1.0195
Schofield O, Saba G, Coleman K et al (2017) Decadal variability in coastal phytoplankton community composition in a changing West Antarctic Peninsula. Deep Sea Res Part I Oceanogr Res Pap 124:42–54. https://doi.org/10.1016/j.dsr.2017.04.014
Scott FJ, Marchant HJ (2005) Cryptophytes. In: Scott FJ, Marchant HJ (eds) Antarctic marine protists. Goanna Print, Canberra, pp 317–318
Smith RC, Martinson DG, Stammerjohn SE et al (2008) Bellingshausen and western Antarctic Peninsula region: pigment biomass and sea-ice spatial/temporal distributions and interannual variabilty. Deep Sea Res Part II Top Stud Oceanogr 55:1949–1963. https://doi.org/10.1016/j.dsr2.2008.04.027
Stoecker DK, Buck KR, Putt (1992) Changes in the sea-ice brine community during the spring-summer transition, McMurdo Sound, Antarctica. I. Photosynthetic protists. Mar Ecol Prog Ser 84:265–278
Sun J, Liu D (2003) Geometric models for calculating cell biovolume and surface area for phytoplankton. J Plankton Res 25:1331–1346. https://doi.org/10.1093/plankt/fbg096
Taylor DL, Lee CC (1971) A new cryptomonad from antarctica: *cryptomonas cryophila sp. nov*. Arch Mikrobiol 75:269–280. https://doi.org/10.1007/BF00407688
Thomson PG, Mcminn A, Kiessling I et al (2006) Composition and succession of dinoflagellates and chrysophytes in the upper fast ice of Davis Station, East Antarctica. Polar Biol 29:337–345. https://doi.org/10.1007/s00300-005-0060-y
Utermöhl H (1958) Zur Vervollkommnung der quantitativen Phytoplankton-Methodik. SIL Commun 1953–1996(9):1–38. https://doi.org/10.1080/05384680.1958.11904091
van den Hoff J, Bell E (2015) The ciliate *Mesodinium rubrum* and its cryptophyte prey in Antarctic aquatic environments. Polar Biol 38(8):1305–1310
Varela M, Fernandez E, Serret P (2002) Size-fractionated phytoplankton biomass and primary production in the Gerlache and south Bransfield Straits (Antarctic Peninsula) in Austral summer 1995–1996. Deep Sea Res Part II Top Stud Oceanogr 49:749–768. https://doi.org/10.1016/S0967-0645(01)00122-9
Vernet M (1992) RACER: predominance of cryptomonads and diatoms in the Gerlache Strait. Antarct J US 27:157–158
Vernet M, Letelier RM, Karl DM (1991) RACER: phytoplankton growth rates in Northern Gerlache Strait during the spring bloom of 1989. Antarct J United States 26:154–156
Vernet M, Martinson D, Iannuzzi R et al (2008) Primary production within the sea-ice zone west of the Antarctic Peninsula: I—sea ice, summer mixed layer, and irradiance. Deep Sea Res Part II Top Stud Oceanogr 55:2068–2085. https://doi.org/10.1016/j.dsr2.2008.05.021
Yoshine HADA (1970) The protozoan plankton of the Antarctic and Subantarctic seas. JARE scientific reports. Ser. E, Biol 31:1–51
Zingone A, Forlani G, Percopo I, Montresor M (2011) Morphological characterization of *Phaeocystis antarctica* (Prymnesiophyceae). Phycologia 50:650–660. https://doi.org/10.2216/11-36.1